Published in final edited form as:
Contrast Media Mol Imaging. 2012 ; 7(1): 19–25. doi:10.1002/cmmi.459.

Nanoparticle-based PARACEST agents: The quenching effect of silica nanoparticles on the CEST signal from surface conjugated chelates

Osasere M. Evbuomwan[a], **Matthew E. Merritt**[b], **Garry E. Kiefer**[a,c], and **A. Dean Sherry**[a,b,*]
[a]Department of Chemistry, University of Texas at Dallas, P.O. Box 830668, Richardson, Texas 75083

[b]AIRC, UT Southwestern Medical Center, 5323 Harry Hines Blvd, Dallas, Texas 75390

[c]Macrocyclics Inc., 1309 Record Crossing, Dallas, Texas 75235

Abstract

Silica nanoparticles of average diameter 53 ± 3 nm were prepared using standard water-in-oil microemulsion methods. After conversion of the surface Si-OH groups to amino groups for further conjugation, the PARACEST agent, EuDOTA-$(gly)_4^-$ was coupled to the amines *via* one or more side-chain carboxyl groups in an attempt to trap water molecules in the inner-sphere of the complex. Fluorescence and ICP analyses showed that ~1200 Eu^{3+} complexes were attached to each silica nanoparticle, leaving behind excess protonated amino groups. CEST spectra of the modified silica nanoparticles showed that attachment of the EuDOTA-$(gly)_4^-$ to the surface of the nanoparticles did not result in a decrease in water exchange kinetics as anticipated but rather resulted in a complete elimination of the normal Eu^{3+}-bound water exchange peak and broadening of the bulk water signal. This observation was traced to catalysis of proton exchange from the Eu^{3+}-bound water molecule by excess positively charged amino groups on the surface of the nanoparticles.

Keywords

Silica nanoparticles; MRI; PARACEST agents; water exchange

1. INTRODUCTION

Chemical exchange saturation transfer (CEST) agents are an emerging class of contrast enhancement media for magnetic resonance imaging (MRI) that offer an alternative to relaxivity-based contrast agents. The major advantage of CEST agents is that one can switch the image contrast “on” and “off” *via* the external application of a radio frequency (RF) presaturation pulse, a feature not available with conventional T_1-based agents that require acquisition of pre- and post- contrast images. Characteristic of all CEST agents is the presence of labile protons (-NH, -OH) or paramagnetically-shifted bound water molecules that exchange into the bulk water pool. This is the origin of their unique image contrast effects. However, to observe CEST, the rate of exchange (k_{ex}) of labile protons (pool A) into

*Correspondence to Advanced Imaging Research Center, UT Southwestern Medical Center, 5323 Harry Hines Blvd, Dallas, Texas 75390, USA. sherry@utdallas.edu; dean.sherry@utsouthwestern.edu.

Supporting Information. Calculation for the determination of number of Eu^{3+} chelates per nanoparticle and CEST spectra of a 2.25 mM EuDOTA-$(gly)_4^-$ solution and a mixture of unmodified silica nanoparticles and 2.25 mM EuDOTA-$(gly)_4^-$.

the bulk water (pool B) must not exceed the chemical shift difference ($\Delta\omega$) between these two chemical environments. This condition allows a discrete spectral difference between water and the exchanging pool thereby permitting activation of one site using a frequency-selective RF presaturation pulse (1).

Early reports showed that numerous low molecular weight compounds including amino acids, sugars, nucleotides, and even intrinsic metabolites were capable of producing CEST contrast (1,2). The chemical shifts of the exchanging components in these compounds are typically not that different from water itself ($\Delta\omega \leq 5$ ppm) so this makes it difficult to saturate at the exchanging site without indirect saturation of bulk water as well. Molecules that display larger chemical shift differences are more attractive as potential CEST agents for two reasons; first, they allow more selective activation at the exchanging site without indirectly affecting the water signal and second, they open the possibility of using faster exchanging systems while still meeting the CEST requirement, $\Delta\omega*\tau_M > 1$. This could in principle increase their contrast sensitivity.

A new class of large $\Delta\omega$ agents became available with the discovery that certain lanthanide ion complexes with DOTA-tetraamide ligands display slow enough water exchange kinetics to meet the CEST requirement. Often, water exchange in these complexes is so slow that a lanthanide-bound water signal can be seen in their high resolution ^{1}H NMR spectra. Complexes of this type are now referred to as PARACEST agents (3,4). Since that original discovery, several laboratories have reported biologically-responsive PARACEST agents for sensing pH (5), temperature (6), metal ions (7), enzyme activity (8,9) and small molecule metabolites (10-13). Since the lanthanide ions display widely variable hyperfine shifts, one can potentially use these systems for multiplex imaging applications since each lanthanide chelate will have a unique activation frequency (14).

Despite these many advantages, current PARACEST agents are relatively insensitive as imaging agents, typically requiring agent concentrations in the mM range. Approaches for increasing CEST sensitivity have included optimizing the proton or water exchange rates and increasing the number of exchangeable groups per agent with the latter approach appearing to be more promising at this point (15-19). Amplification schemes based on nanoparticles of various types are also attractive since nanoparticles can entrap a high concentration of exchangeable groups in their internal cavities or provide a large surface area for delivery of a high payload of contrast agent to a specific site of interest.

The first class of nano-sized systems used for CEST involved the entrapment of a large number of paramagnetic chelates within the cavity of a liposome (20) and apoferritin (21). While liposome-based systems can be detected in the picomolar range, entrapment of PARACEST agents in the cavity of apoferritin was completely ineffective due to catalysis of water protons exchange by interior charged surface residues of the protein. A second class of nano-sized systems was designed to exploit the high surface area of nanoparticles by modifying the surface of perfluorocarbon droplets (22) or virus nanoparticles (23) with PARACEST agents. In both cases, an 11-12 % decrease in water signal was observed upon saturation at the CEST exchange frequency in these systems. These observations thus suggest that the location of the agent (in an inner cavity versus on the surface of a nanoparticle) and the material used in the fabrication of the nanoparticle could both impact the CEST properties of the resulting nanoparticles.

In an effort to further explore alternate nanoparticle constructs that might enhance the sensitivity of PARACEST agents, we report here the covalent attachment of a well characterized agent, EuDOTA-$(gly)_4^-$ (Figure 1) to silica nanoparticles *via* conjugation of one or more side-chain carboxyl groups to surface amino groups. Silica nanoparticles were

selected for this study due to the abundance of available silanol groups for modification and agent attachment as well as the reported chemical inertness of silica (24). Given that water exchange in EuDOTA-$(gly)_4^-$ is faster than optimal for CEST (25), it is important to find ways to slow water exchange even further. In principle, if one could link all four carboxyl groups of the complex to the nanoparticle surface, this could hinder dissociation of the Eu^{3+}-bound water molecule even further and thereby enhance the CEST contribution from each europium center. Combining this with the amplification effect of having multiple agents on a single nanoparticle would substantially increase the CEST sensitivity of each nanoparticle.

2. RESULTS AND DISCUSSION

2.1. Synthesis and surface modification of silica nanoparticles

Silica nanoparticles have been used in a wide range of applications including immunoassays (26), cell labeling (27), bacterial detection (28), nucleic acid delivery (29), optical imaging (30), and magnetic resonance imaging (31). The versatility of silica nanoparticles stems from the abundance of silanol groups on their surface and the commercial availability of a wide range of silane coupling agents for modification of the surface silanol groups (32). Silica nanoparticles have been synthesized using a variety of methods but the water-in-oil microemulsion (33) is preferred for preparing nanoparticles of uniform size. A microemulsion is an isotropic, thermodynamically stable, single-phase system consisting of three components; water, oil and a surfactant that forms reverse micelles. Reverse micelles consist of nanodroplets of water surrounded and stabilized by the surfactant and these nanodroplets serve as the reaction chamber for synthesis of uniform sized silica nanoparticles *via* base catalyzed hydrolysis and polycondensation of an alkoxysilane (34). The resulting nanoparticles are spherical and contain free surface silanol groups for further modification. In this study, 3-aminopropyl-triethoxysilane (APTS) was used to introduce amine groups onto the silica nanoparticle surface. This hydrolysis/condensation reaction introduces a large number of amine groups on the surface of the nanoparticle for subsequent conjugation with other agents or reporter molecules. The EDC/sulfo-NHS technique (35) was used to attach EuDOTA-$(gly)_4^-$ onto the nanoparticle surface *via* formation of amide linkages with the surface amino groups. The preformed complex was used as reactant instead of free ligand to insure that every attached macrocycle contained a Eu^{3+} ion and to avoid any non-specific binding of Eu^{3+} ions to negatively charged surface silanol groups if the Eu^{3+} was added after ligand conjugation.

2.2. TEM Imaging

Nanoparticles were observed to be spherical in shape and highly monodisperse by TEM (Figure 2). The average diameters of the unmodified, amine-modified, and EuDOTA-$(gly)_4^-$ modified silica nanoparticles were 53 ± 3 nm, 53 ± 4 nm, and 55 ± 3 nm, respectively. No difference in morphology was observed among the three types of nanoparticles. These data indicate that surface modification did not significantly affect the structure or size of the nanoparticles. Furthermore, the size similarity suggests that the conjugated complex forms only a thin layer on the nanoparticle surface.

2.3. Analysis of surface amine groups and surface-bound EuDOTA-$(gly)_4^-$ complexes

The presence of amine groups was confirmed by reaction of the nanoparticles with fluorescamine, a non-fluorescent reagent which reacts with primary amines at room temperature to produce a highly fluorescent derivative. This reagent permits highly sensitive analyses of substances containing amine functionalities (picomolar range) and can be used in both solid and liquid phases (36).

Intense fluorescence was observed for the amine-modified silica nanoparticles after reaction with fluorescamine and this demonstrated that the amino groups on the surface were accessible for further reaction. A decrease in fluorescence was observed after covalent attachment of EuDOTA-$(gly)_4^-$ which was consistent with a reduction in the number of free amino groups after conjugation. Using a standard calibration curve, the fluorescence intensity differences between these two samples allowed an estimate of the number of amino groups that had reacted with EuDOTA-$(gly)_4^-$ at 12.3 nmol/mg of nanoparticle. This value reflects ~36% of the total amino groups originally present on the surface so by difference, one can conclude that ~64% of the amino groups (21.7 nmol/mg) did not form a conjugate. ICP data confirmed that there was indeed Eu^{3+} on the surface of the nanoparticles at a concentration of 12 nmol/mg nanoparticle. The agreement between these two independent analyses indicates that each Eu^{3+} complex was, on average, attached *via* a single carboxyl group. These data translate to about 1200 molecules of EuDOTA-$(gly)_4^-$ per nanoparticle (see supporting information), a number that is coincidently very similar to the number of Tm^{3+}-based PARACEST agents attached to adenovirus particles reported in a previous study (23).

2.4. CEST studies

CEST spectra were collected by applying a frequency-selective presaturation pulse in small steps over a large frequency range and plotting the residual bulk water signal intensity, M_s / M_o, as a function of saturation frequency. The CEST spectrum of a 2.25 mM aqueous solution of EuDOTA-$(gly)_4^-$ (black circles, Figure 3a) shows the typical Eu^{3+}-bound water exchange peak near 50 ppm. A fit of this spectrum to the Bloch equations for three site exchange (Eu^{3+}-water molecule, four equivalent ligand amide –NH protons, and bulk water protons) provided a Eu^{3+}-bound water molecule lifetime of 128 μs and a –NH proton exchange lifetime of 17.5 ms. A separate –NH exchange peak is not observed here because the chemical shift of the –NH protons in the complex is very close to water itself.

The red curve in Figure 3a represents the CEST spectrum of a suspension of SiO_2-NPs having an equivalent amount of EuDOTA$(gly)_4^-$ (2.25 mM) covalently attached to the nanoparticle surface. This CEST spectrum showed no hint of a Eu^{3+}-bound water exchange peak near 50 ppm but rather appeared as a broad exchange peak with a shape reminiscent of a tissue magnetization transfer (MT) signal (37). This shape can be mimicked experimentally by a variety of semi-solids suspended in water such as agarose and alginates and represents water proton dipoles that are not averaged by molecular motions in the magnetic field.

The absence of a distinct exchange peak from surface-bound EuDOTA-$(gly)_4^-$ suggests that water exchange in this system is either too fast or too slow for CEST detection. The pronounced broadening of the spectrum is most consistent with rapid proton exchange between multiple proton donors on the nanoparticle surface, perhaps including the paramagnetic agent and any remaining unreacted primary amino groups (21.7 nmol / mg of nanoparticle). To check whether the excess surface amino groups on the SiO_2-NPs contribute significantly to the shape of the broad MT-like signal, CEST spectra of unmodified SiO_2-NPs containing only Si-OH exchanging protons and SiO_2-NPs containing excess amino groups (no Eu^{3+}-bound agent) were also compared (Figure 3b). Here, both types of SiO_2-NPs give a broad MT-type signal but the SiO_2-NP sample having surface amino groups shows a substantially broader profile. This indicates that the exchanging amino protons do contribute to the CEST profile above and beyond the effects due to dipolar coupling (MT effect).

In an attempt to better understand the influence of the surface functional groups on the CEST properties of EuDOTA-$(gly)_4^-$, titrations were performed by adding either

poly(allylamine hydrochloride) (PAH) or poly(acrylic acid) (PAA) to a solution of 2.25 mM EuDOTA-$(gly)_4^-$ while recording CEST spectra after each addition. These particular polymers were chosen because they would introduce a large number of positive or negatively charged functional groups by using macromolecules that have enough motional flexibility to allow complete dipolar averaging.

Figures 4a and b display CEST spectra collected before and after addition of small amounts of the polymers, PAH or PAA, to a 2.25 mM solution of EuDOTA-$(gly)_4^-$. Addition of PAH resulted in quenching of the Eu^{3+}-bound water exchange peak and broadening of the bulk water resonance. Both effects are consistent with acceleration of water proton exchange between the Eu^{3+}-bound water molecule and bulk water solvent. In comparison, addition of PAA to another sample of EuDOTA-$(gly)_4^-$ had essentially no effect on the Eu^{3+}-water exchange CEST signal. These observations illustrate that the presence of the PAH amino protons alone in the same solution as the agent has a substantial impact on the water proton exchange rate from the Eu^{3+} centers (Figure 4a). Conversely, an equivalent number of excess carboxyl groups had little to no impact on Eu^{3+}-water exchange kinetics (Figure 4b). The most reasonable explanation is that EuDOTA-$(gly)_4^-$ forms a strong ion-pair with the positively charged amino groups of PAH which likely brings the charged amino groups near the Eu^{3+}-bound water molecule to establish a local hydrogen-bonding network of proton donor/acceptors and this results in proton catalyzed exchange much like that observed previously in the pH sensitive gadolinium complex, GdDOTA-4AmP^{5-}, as the extended phosphonate groups become protonated (38). Interestingly, this catalytic process seems to occur regardless of whether the EuDOTA-$(gly)_4^-$ complex is covalently attached to a macromolecule (as illustrated by the SiO_2-NP results) or whether they are simply mixed together in aqueous solution (as illustrated by the EuDOTA-$(gly)_4^-$/PAH mixture).

To further confirm this hypothesis, a Bloch simulation of the CEST spectrum of the EuDOTA-$(gly)_4^-$/PAH mixture was performed (Figure 4a). A fit of the experimental CEST spectrum of EuDOTA-$(gly)_4^-$ alone (Figure 3a) gave a Eu^{3+}-bound water lifetime (τ_M) of 128 μs, typical of a slow water exchange complex. If one adds a 10-fold excess of amino groups (over the Eu^{3+} concentration) and allows each amino proton to exchange at a typical exchange rate of 4000 s^{-1} at pH 7.0 (1) while fixing the Eu(III)-bound water lifetime to 128 μs, the CEST spectrum of Figure 5 could not be reproduced (the Eu^{3+}-bound water resonance was still visible). However, by allowing catalytic prototropic exchange between the Eu^{3+}-bound and bulk water molecule to increase 10-fold (τ_M = 12.5 μs) while keeping all other parameters constant, a nearly perfect replication of the CEST spectrum was achieved. This provides further support to our hypothesis that the presence of amine groups in the vicinity of a Eu^{3+}-bound water molecule results in catalysis of proton exchange by about 10-fold. This result is similar to the observation reported by Vasalatiy *et al.*(21) who found that the CEST signal arising from a slow-water exchange complex, the ethyl ester of EuDOTA-$(gly)_4^-$, disappeared upon encapsulation of this complex in the interior of apoferritin. Similar to the results illustrated here, this was attributed to enhanced prototropic exchange catalyzed by charged groups on the inner surface of the protein core.

3. CONCLUSIONS

In this work, silica nanoparticles were prepared using microemulsions techniques and ~1200 EuDOTA-$(gly)_4^-$ molecules were attached to each nanoparticle *via* conjugation of agent carboxyl groups to surface amines. The CEST properties of the modified nanoparticles showed that surface conjugation of the paramagnetic agent did not decrease the Eu^{3+}-bound water exchange rate as we had hoped but rather resulted in complete elimination of the water exchange signal. This observation was traced to enhanced proton exchange due to ion-pair interactions between EuDOTA-$(gly)_4^-$ and the excess amino protons on the nanoparticle

surface. These results demonstrate that silica nanoparticles having excess protonated amino groups on their surface are poor candidates as an amplifying platform for EuDOTA-$(gly)_4^-$ for targeted imaging applications. However, it may be possible to identify other PARACEST agents where the lanthanide-bound water molecule is sequestered enough within the structure to protect it from external functional groups that efficiently catalyze proton exchange.

4. EXPERIMENTAL

4.1. General

All reagents and solvents were purchased from commercial sources and used as received, unless otherwise stated. Millipore deionized (DI) water was used in all instances that required water.

4.2. Synthesis of EuDOTA-$(gly)_4^-$

EuDOTA-$(gly)_4^-$ was synthesized according to previously described methods (3).

4.3. Synthesis and amine-modification of silica nanoparticles

Silica nanoparticles were synthesized using a previously described water-in-oil microemulsion method (39). The surface Si-OH groups were further modified by suspending 200 mg of the nanoparticles in a 20 mL ethanol solution containing 400 μL of (3-aminopropyl)triethoxysilane (APTS). After 18 h, the amine-modified nanoparticles were isolated from the mixture by centrifugation at 3750 rpm and washed multiple times in ethanol and water to remove the excess organosilane.

4.4. Conjugation of EuDOTA-$(gly)_4^-$ to amine-modified silica nanoparticles

100 mg of amine-modified silica nanoparticles was suspended in 15 mL of 10 mM phosphate buffer (pH 7.4) at 0°C. $[EuDOTA\text{-}(gly)_4]^-$ (65 mg, 0.083 mmol), N-hydroxysulfosuccinimide sodium salt (72 mg, 0.332 mmol), and N-(3-dimethylaminopropyl)-N'-ethylcarbodiimide hydrochloride (64 mg, 0.332 mmol), were added to the reaction mixture which was allowed to warm up to room temperature and stirred for 18 h. The modified nanoparticles were separated from the reaction mixture by centrifugation at 3750 rpm and washed multiple times with water to remove any excess reagent.

4.5. Transmission electron microscopy (TEM) and size characterization

Nanoparticle size was characterized by transmission electron microscopy (TEM) using a JEOL 1200 EX electron microscope operating at an accelerating voltage of 120 kV and a resolution of 0.34 nm. The samples were prepared by placing 10 μL of a 0.1 mg/mL nanoparticle/ethanol suspension on a carbon-coated copper grid and drying in air. The average nanoparticle diameter was measured with the aid of the ITEM software.

4.6. Fluorescamine assay

The presence of amine groups on the silica surface was confirmed by a fluorescamine assay (36). The fluorescamine reagent was prepared by dissolving 2 mg of fluorescamine in 1 mL of acetone. 300 μL of this solution was added to 200 μL of 2 mg/mL nanoparticle suspension prepared in borate buffer (pH 8.5). The resulting fluorescence was measured on a Perkin Elmer LS 50B Luminescence spectrometer using excitation and emission wavelengths of 390 and 485 nm.

4.7. Analysis of the number of surface-bound EuDOTA-$(gly)_4^-$ complexes

The concentration of EuDOTA-$(gly)_4^-$ on the nanoparticle surface was determined by inductively coupled plasma optical emission spectrometry (ICP-OES). This experiment was performed by Galbraith Laboratory Inc. (Knoxville, TN) and the data obtained was used to estimate the number of EuDOTA-$(gly)_4^-$ molecules per nanoparticle.

4.8. CEST spectra

CEST spectra were recorded on a Bruker AVANCE III 400 NMR spectrometer operating at 400.13 MHz. Solutions containing 2.25 mM EuDOTA-$(gly)_4^-$ and a nanoparticle suspension containing an equivalent concentration of Eu^{3+} were analyzed. Control experiments involving the gradual addition of the polymers poly(allylamine hydrochloride) (PAH), 70,000 g/mol and polyacrylic acid (PAA) to a 2.25 mM EuDOTA-$(gly)_4^-$ solution were performed in order to determine the effect of the presence of primary amino groups on the CEST properties of the Europium complex.

4.9. CEST simulations

The experimental CEST spectrum of 2.25 mM EuDOTA-$(gly)_4^-$ plus excess PAH mixture was fitted to the Bloch equation using a program written in MATLAB and the following experimental parameters: Eu-(III)-bound water T_1 = 17.5 ms, bulk water T_1 = 2.5 s, Eu-(III)-bound water lifetime = 128 μs, [Eu-complex] = 2.25 mM, [NH_2 groups] = 10 × [Eu-complex], Saturation frequency = 23.5 μT, and k_{ex} of NH_2 group = 4000 Hz. All parameters were kept constant while the water exchange rate was incrementally increased until good agreement was reached with the experimental CEST spectrum.

Supplementary Material

Refer to Web version on PubMed Central for supplementary material.

Acknowledgments

The authors wish to acknowledge financial support from the National Institutes of Health (RR-02584, CA115531 and EB004582) and the Robert A. Welch Foundation (AT-584). We also thank Drs. Piyu Zhao and Yunkou Wu from UT Dallas and Tom Januszewski and Laurie Mueller from the Molecular and Cellular Imaging Facility at UTSW.

REFERENCES

1. Ward KM, Aletras AH, Balaban RS. A new class of contrast agents for MRI based on proton chemical exchange dependent saturation transfer (CEST). J. Magn. Reson. 2000; 143(1):79–87. [PubMed: 10698648]
2. Guivel-Scharen V, Sinnwell T, Wolff SD, Balaban RS. Detection of proton chemical exchange between metabolites and water in biological tissues. J. Magn. Reson. 1998; 133(1):36–45. [PubMed: 9654466]
3. Zhang S, Wu K, Biewer MC, Sherry AD. 1H and (17)O NMR detection of a lanthanide-bound water molecule at ambient temperatures in pure water as solvent. Inorg. Chem. 2001; 40(17):4284–4290. [PubMed: 11487334]
4. Zhang S, Winter P, Wu K, Sherry AD. A novel europium(III)-based MRI contrast agent. J. Am. Chem. Soc. 2001; 123(7):1517–1518. [PubMed: 11456734]
5. Aime S, Barge A, Castelli DD, Fedeli F, Mortillaro A, Nielsen FU, Terreno E. Paramagnetic lanthanide(III) complexes as pH-sensitive chemical exchange saturation transfer (CEST) contrast agents for MRI applications. Magn. Reson. Med. 2002; 47(4):639–648. [PubMed: 11948724]
6. Zhang SR, Malloy CR, Sherry AD. MRI thermometry based on PARACEST agents. J. Am. Chem. Soc. 2005; 127(50):17572–17573. [PubMed: 16351064]

7. Trokowski R, Ren JM, Kalman FK, Sherry AD. Selective sensing of zinc ions with a PARACEST contrast agent. Angew. Chem. Int. Ed. Engl. 2005; 44(42):6920–6923. [PubMed: 16206314]
8. Yoo B, Pagel MD. A PARACEST MRI contrast agent to detect enzyme activity. J. Am. Chem. Soc. 2006; 128(43):14032–14033. [PubMed: 17061878]
9. Chauvin T, Durand P, Bernier M, Meudal H, Doan BT, Noury F, Badet B, Beloeil JC, Toth E. Detection of enzymatic activity by PARACEST MRI: A general approach to target a large variety of enzymes. Angew. Chem. Int. Ed. Engl. 2008; 47(23):4370–4372. [PubMed: 18454438]
10. Aime S, Delli Castelli D, Fedeli F, Terreno E. A paramagnetic MRI-CEST agent responsive to lactate concentration. J. Am. Chem. Soc. 2002; 124(32):9364–9365. [PubMed: 12167018]
11. Zhang SR, Trokowski R, Sherry AD. A paramagnetic CEST agent for imaging glucose by MRI. J. Am. Chem. Soc. 2003; 125(50):15288–15289. [PubMed: 14664562]
12. Trokowski R, Zhang SR, Sherry AD. Cyclen-based phenylboronate ligands and their Eu3+ complexes for sensing glucose by MRI. Bioconjug. Chem. 2004; 15(6):1431–1440. [PubMed: 15546212]
13. Ren JM, Trokowski R, Zhang SR, Malloy CR, Sherry AD. Imaging the Tissue Distribution of Glucose in Livers Using A PARACEST Sensor. Magn. Reson. Med. 2008; 60(5):1047–1055. [PubMed: 18958853]
14. Aime S, Carrera C, Delli Castelli D, Geninatti Crich S, Terreno E. Tunable imaging of cells labeled with MRI-PARACEST agents. Angew. Chem. Int. Ed. Engl. 2005; 44(12):1813–1815. [PubMed: 15723362]
15. Aime S, Delli Castelli D, Terreno E. Supramolecular adducts between poly-L-arginine and [Tm(III)dotp]: A route to sensitivity-enhanced magnetic resonance imaging-chemical exchange saturation transfer agents. Angew. Chem. Int. Ed. Engl. 2003; 42(37):4527–4529. [PubMed: 14520757]
16. Goffeney N, Bulte JWM, Duyn J, Bryant LH, van Zijl PCM. Sensitive NMR detection of cationic-polymer-based gene delivery systems using saturation transfer via proton exchange. J. Am. Chem. Soc. 2001; 123(35):8628–8629. [PubMed: 11525684]
17. Pikkemaat JA, Wegh RT, Lamerichs R, van de Molengraaf RA, Langereis S, Burdinski D, Raymond AYF, Janssen HM, de Waal BFM, Willard NP, Meijer EW, Grull H. Dendritic PARACEST contrast agents for magnetic resonance imaging. Contrast Media Mol. Imaging. 2007; 2(5):229–239. [PubMed: 17937448]
18. Snoussi K, Bulte JWM, Gueron M, van Zijl PCM. Sensitive CEST agents based on nucleic acid imino proton exchange: Detection of poly(rU) and of a dendrimer-poly(rU) model for nucleic acid delivery and pharmacology. Magn. Reson. Med. 2003; 49(6):998–1005. [PubMed: 12768576]
19. Wu YK, Zhou YF, Ouari O, Woods M, Zhao PY, Soesbe TC, Kiefer GE, Sherry AD. Polymeric PARACEST agents for enhancing MRI contrast sensitivity. J. Am. Chem. Soc. 2008; 130(42): 13854–13855. [PubMed: 18817395]
20. Aime S, Castelli DD, Terreno E. Highly sensitive MRI chemical exchange saturation transfer agents using liposomes. Angew. Chem. Int. Ed. Engl. 2005; 44(34):5513–5515. [PubMed: 16052647]
21. Vasalatiy O, Zhao P, Zhang S, Aime S, Sherry AD. Catalytic effects of apoferritin interior surface residues on water proton exchange in lanthanide complexes. Contrast Media Mol Imaging. 2006; 1(1):10–14. [PubMed: 17193595]
22. Winter PM, Cai KJ, Chen J, Adair CR, Kiefer GE, Athey PS, Gaffney PJ, Buff CE, Robertson JD, Caruthers SD, Wickline SA, Lanza GM. Targeted PARACEST nanoparticle contrast agent for the detection of fibrin. Magn. Reson. Med. 2006; 56(6):1384–1388. [PubMed: 17089356]
23. Vasalatiy O, Gerard RD, Zhao P, Sun XK, Sherry AD. Labeling of adenovirus particles with PARACEST agents. Bioconjug. Chem. 2008; 19(3):598–606. [PubMed: 18254605]
24. Smith JE, Wang L, Tan WT. Bioconjugated silica-coated nanoparticles for bioseparation and bioanalysis. Trends Analyt. Chem. 2006; 25(9):848–855.
25. Dixon WT, Ren JM, Lubag AJM, Ratnakar J, Vinogradov E, Hancu I, Lenkinski RE, Sherry AD. A Concentration-Independent Method to Measure Exchange Rates in PARACEST Agents. Magn. Reson. Med. 2010; 63(3):625–632. [PubMed: 20187174]

26. Santra S, Zhang P, Wang KM, Tapec R, Tan WH. Conjugation of biomolecules with luminophore-doped silica nanoparticles for photostable biomarkers. Anal. Chem. 2001; 73(20):4988–4993. [PubMed: 11681477]
27. He XX, Duan JH, Wang KM, Tan WH, Lin X, He CM. A novel fluorescent label based on organic dye-doped silica nanoparticles for HepG liver cancer cell recognition. J. Nanosci. Nanotechnol. 2004; 4(6):585–589. [PubMed: 15518391]
28. Zhao XJ, Hilliard LR, Mechery SJ, Wang YP, Bagwe RP, Jin SG, Tan WH. A rapid bioassay for single bacterial cell quantitation using bioconjugated nanoparticles. Proc. Natl. Acad. Sci. U. S. A. 2004; 101(42):15027–15032. [PubMed: 15477593]
29. Kneuer C, Sameti M, Bakowsky U, Schiestel T, Schirra H, Schmidt H, Lehr CM. A nonviral DNA delivery system based on surface modified silica-nanoparticles can efficiently transfect cells in vitro. Bioconjug. Chem. 2000; 11(6):926–932. [PubMed: 11087343]
30. Kumar R, Roy I, Hulchanskyy TY, Goswami LN, Bonoiu AC, Bergey EJ, Tramposch KM, Maitra A, Prasad PN. Covalently dye-linked, surface-controlled, and bioconjugated organically modified silica nanoparticles as targeted probes for optical imaging. ACS Nano. 2008; 2(3):449–456. [PubMed: 19206569]
31. Taylor KML, Kim JS, Rieter WJ, An H, Lin WL, Lin WB. Mesoporous silica nanospheres as highly efficient MRI contrast agents. J. Am. Chem. Soc. 2008; 130(7):2154–2155. [PubMed: 18217764]
32. Wang L, Wang KM, Santra S, Zhao XJ, Hilliard LR, Smith JE, Wu JR, Tan WH. Watching silica nanoparticles glow in the biological world. Anal. Chem. 2006; 78(3):646–654.
33. Bagwe RP, Yang CY, Hilliard LR, Tan WH. Optimization of dye-doped silica nanoparticles prepared using a reverse microemulsion method. Langmuir. 2004; 20(19):8336–8342. [PubMed: 15350111]
34. El-Nahhal IM, El-Ashgar NM. A review on polysiloxane-immobilized ligand systems: Synthesis, characterization and applications. J. Organomet. Chem. 2007; 692(14):2861–2886.
35. Hermanson, GT. Bioconjugate techniques. Academic Press; San Diego: 1996. p. xxvp. 785
36. Udenfriend S, Stein S, Bohlen P, Dairman W. Fluorescamine - Reagent for Assay of Amino-Acids, Peptides, Proteins, and Primary Amines in Picomole Range. Science. 1972; 178(4063):871–872. [PubMed: 5085985]
37. Wolff SD, Balaban RS. Magnetization transfer contrast (MTC) and tissue water proton relaxation in vivo. Magn. Reson. Med. 1989; 10(1):135–144. [PubMed: 2547135]
38. Zhang SR, Wu KC, Sherry AD. A novel pH-sensitive MRI contrast agent. Angew. Chem. Int. Ed. Engl. 1999; 38(21):3192–3194. [PubMed: 10556899]
39. Bagwe RP, Hilliard LR, Tan WH. Surface modification of silica nanoparticles to reduce aggregation and nonspecific binding. Langmuir. 2006; 22(9):4357–4362. [PubMed: 16618187]

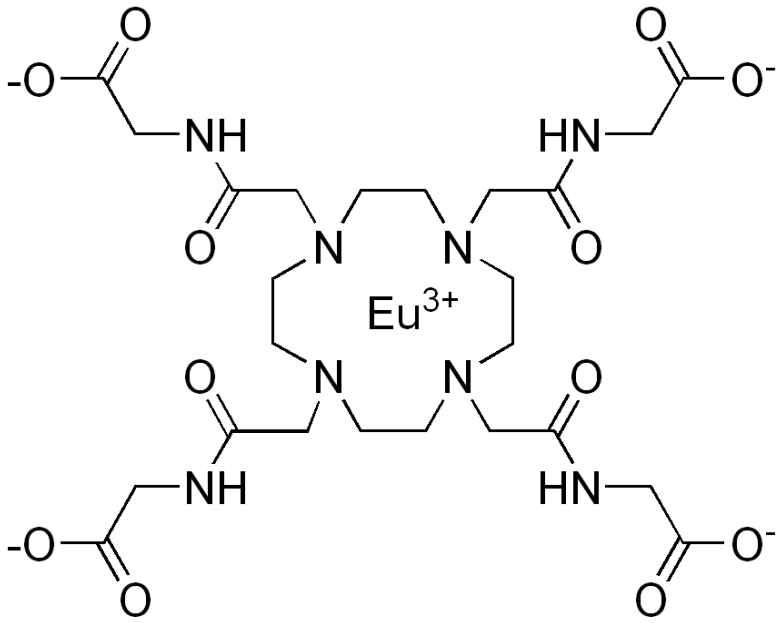

Figure 1.
Chemical structure of EuDOTA-$(gly)_4^-$

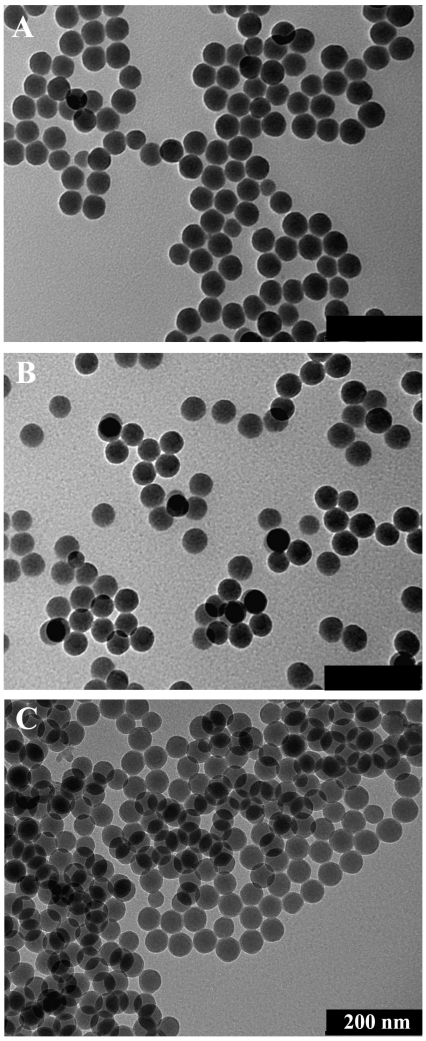

Figure 2.
Transmission electron micrographs of (a) unmodified, (b) amine-modified, and (c) EuDOTA-$(gly)_4^-$modified silica nanoparticles. Scale Bar = 200 nm

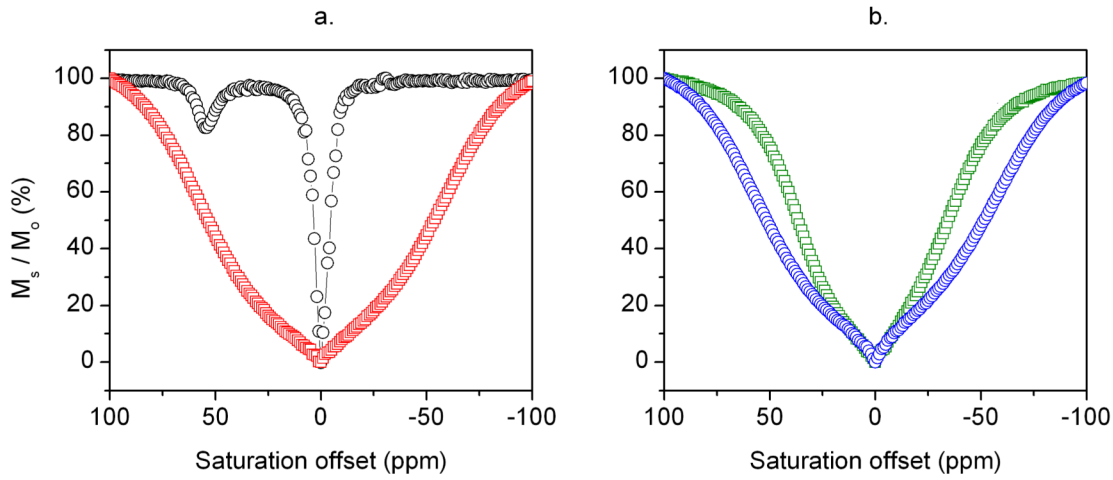

Figure 3.

(a) CEST spectra of 2.25 mM aqueous solution of EuDOTA-$(gly)_4^-$ (black circles) and a nanoparticle suspension containing 2.25 mM of surface-bound EuDOTA-$(gly)_4^-$ (red squares). (b) CEST spectra of unmodified SiO_2-NPs (green squares) and amine-modified SiO_2-NPs (blue circles) nanoparticle suspensions. The spectra were recorded at 25°C and pH 7 using a presaturation pulse of 23.5 μT and saturation time of 3 s. M_s/M_o refers to the ratio of the bulk water signal intensity in the presence (M_s) and absence (M_o) of the presaturation pulse.

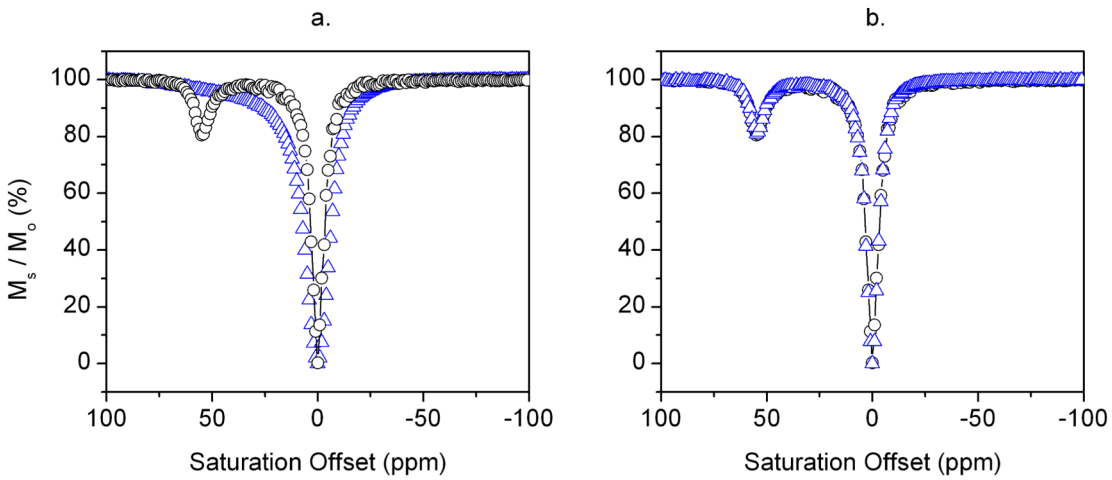

Figure 4.

(a) CEST Spectra of an aqueous solution of 2.25 mM EuDOTA-$(gly)_4^-$ (black circles), and a mixture of 2.25 mM EuDOTA-$(gly)_4^-$ and 6 mg PAH (blue triangles). (b) CEST Spectra of an aqueous solution of 2.25 mM EuDOTA-$(gly)_4^-$ (black circles), and a mixture of 2.25 mM EuDOTA-$(gly)_4^-$ and 6 mg PAA (blue triangles). The spectra were recorded at 25°C and pH 7 using a presaturation pulse of 23.5 μT and saturation time of 3 s.

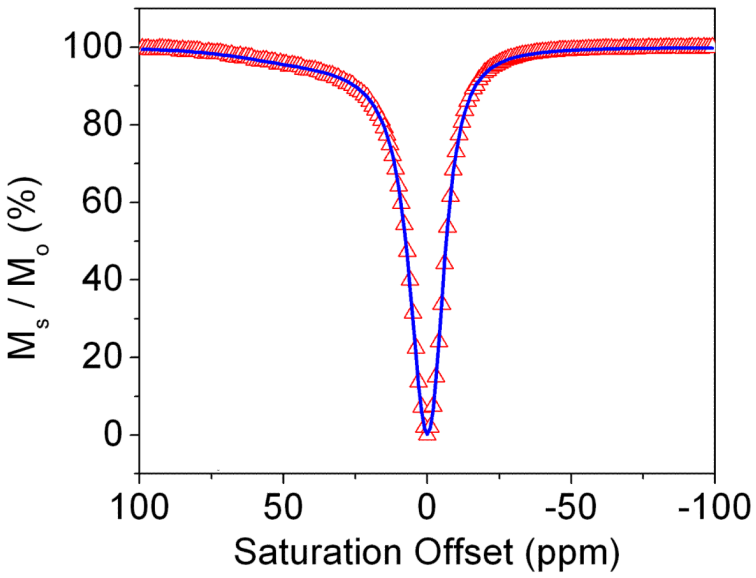

Figure 5.
CEST spectra of a mixture of 2.25 mM EuDOTA-$(gly)_4^-$ and 6 mg PAH (red triangles) and a simulation of the PAH data (blue line) using the exchange rates and other parameters described in the experimental section.